Laminar Rayleigh-Bénard Convection in Perfectly Conducting Curvilinear Cavities

R. Haj Mohamad[1], A.Mourtada[1], X. Chesneau[2] and B. Zeghmati [2]

[1] Faculty of Engineering III, Lebanese University, Hadeth Beirut, Lebanon
[2] Laboratoire de Mathématiques et Physique des Systèmes, Groupe de Mécanique Énergétique, Université de Perpignan, 52 Avenue Paul Alduy, 66860 Perpignan cedex, France
Email : hrami73@hotmail.com

Abstract

A numerical work carries on flow structures and heat transfer rates generated by Rayleigh-Bénard convective motions of Boussinesq fluid with a Prandtl number of 0.7 in a perfectly conducting curvilinear cavities of aspect ratios : $1 \leq L_x \leq 5$, $1 \leq L_y \leq 10$. Transfer equations based on Boussinesq approximation are solved by using the FLEXPDE software. The heating rate, introduced through a time dependent Rayleigh number Ra, drives a flow transition in the range of supercritical Rayleigh numbers : $10^3 \leq Ra \leq 10^6$. The flow pattern starts of a single, symmetric circulation cell for low Rayleigh number, but highly mixed , thermally stratified two-dimensional flow and the circulation cell undergoes cross-sectional changes in high range of Rayleigh number. Numerical values of the Nusselt number as a function of the Rayleigh number and the cavity aspect ratio are reported. The influence of the dimensionless distance between the heated plate and the cooled sides on the average Nusselt number < Nu > is more significant for the system with a smaller Ra.

Résumé : Une étude numérique de la convection naturelle de type Rayleigh –Bénard dans une enceinte demi-cylindrique remplie d'air est présentée. La paroi supérieure de cette enceinte est soumise à un flux de chaleur uniforme de densité constante et l'autre paroi est refroidie par un flux uniforme de densité constante. Les transferts dans l'enceinte sont décrits par les équations classiques de la convection naturelle écrites dans un référentiel cartésien. Ces équations basées sur l'approximation de Boussinesq sont résolues en utilisant le code industriel FLEXPDE Nous analysons l'influence des rapports de forme de l'enceinte ($1 \leq L_x \leq 5$, $1 \leq L_y \leq 10$.) et du nombre de Rayleigh ($10^3 \leq Ra \leq 10^6$) sur la structure de l'écoulement et les transferts de chaleur. Les résultats montrent notamment que la structure de l'écoulement est décrite, pour les faibles nombres de Rayleigh, par deux cellules contrarotatives. L'influence du rapport de forme de l'enceinte Lx / Ly sur le nombre de Nusselt < Nu > et la valeur maximale de la fonction de courant augmente avec le nombre de Rayleigh.

Keywords: Rayleigh-Bénard convection; Curvilinear Cavities; Stream function, isotherm, Nussel number.

Nomenclature

g	gravitational acceleration (m s^{-2})
k	thermal conductivity (W m^{-1} K^{-1})
L_x	cavity half length (m)
L_y	cavity height (m)
Nu	local Nusselt number
<Nu>	overall Nusselt number
Pr	Prandtl number
$q_{1,2}$	heat flux density , (W m^{-2})
Ra	Rayleigh number, $g\beta L_y^4 q_1/\nu \alpha k$
Ra(t)	time dependent Rayleigh number (Ra / τ) t
T	Temperature (K)
ΔT	difference temperature, (q_1 L_y / k) (K)
t	time (s)
u, v	velocity components at x, y coordinates respectively (m s^{-1})
U, V	dimensionless velocity components at X, Y coordinates respectively
x, y	Cartesian coordinates (m)
X, Y	dimensionless Cartesian coordinates

Greek symbols

α	thermal diffusivity (m^2 s^{-1})
β	thermal expansion coefficient (K^{-1})
ξ	dimensionless vorticity
Θ	dimensionless temperature
Ψ	dimensionless stream function
τ	dimensionless duration of the unsteady heating

1. Introduction

Rayleigh-Bénard (RB) convection is taking considerable importance since it is related to some of the flow phenomena in many practical situations, such as cooling of electronic equipment by natural convection, thermal comfort in buildings, heat loss from solar collector and crystal growth. RB Convection has been extensively investigated [1-8] inside box cavities and cylindrical containers because of the geometrical simplicity of the boundary conditions. Yang [2] analyzed laminar buoyant flows in confined enclosures heated from below and cooled up side while the horizontal sides are adiabatic. They found that the buoyancy forces generated by imposed condition drive a rising flow near these walls, independently of the Rayleigh number. However, a pure conductive regime is dominant until the critical Rayleigh number is reached. Then the convective patterns starts independently of the final supercritical Rayleigh number. Thus, they concluded a competition of buoyancy forces generated near side walls against those In the present work, the governing equations for a Boussinesq fluid of Prandtl number Pr = 0.71 are solved numerically in a curvilinear cavities of aspect ratios $1 \leq L_x \leq 5$, $1 \leq L_y \leq 10$. cavities are heated upside and symmetrically cooled from curved sides while a linear time dependent Rayleigh number Ra function is considered. The space-time evolution of temperature, stream function depending on the Rayleigh numbers and the cavities aspect ratios are shown.

2. Mathematical Formulation

The top wall, is prescribed by positive heat flux q_1, while the curved walls are prescribed by output heat flux q_2. The 2-D natural convection flows are assumed to be unsteady and laminar. Consider a curvilinear cavity of height L_y and length $2L_x$ filled with a Boussinesq fluid of Prandtl number Pr = 0.71 (Figure 1). The Boussinesq approximation is adopted and the equations representing the conversation of momentum, mass and energy for unsteady motion can be written in stream function-vorticity form as:

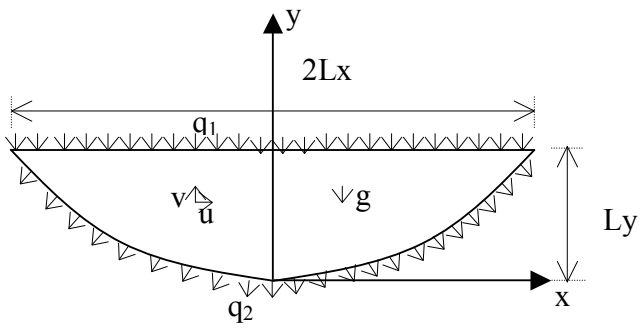

Figure 1: Physical model and coordinates system

$$\frac{\partial \xi}{\partial t} + Pr^{-1}\left(U\frac{\partial \xi}{\partial X} + V\frac{\partial \xi}{\partial Y}\right) = \nabla^2 \xi + Ra\frac{\partial \Theta}{\partial X} \quad (1)$$

$$\nabla^2 \Psi + \xi = 0 \quad (2)$$

$$\frac{\partial \Theta}{\partial t} + U\frac{\partial \Theta}{\partial X} + V\frac{\partial \Theta}{\partial Y} = \nabla^2\ \Theta \quad (3)$$

$$\text{with } (X, Y) = (x, y) / L_y,\ (U, V) = (u, v) / (\alpha / L_y),\ \Theta = (T - T_c) / \Delta T,\ t = t'\alpha / L_y^2 \quad (4)$$

No-slip condition is applied to the velocity Boundary Conditions (BCs) for all the walls, the corresponding (BCs) are:

$$\text{At } Y = 0, -\Gamma_X \le X \le \Gamma_X, -\frac{\partial \Theta}{\partial Y} = \text{ltp},\ \Psi = \frac{\partial \Psi}{\partial Y} = 0 \quad (5)$$

$$\text{For } -\Gamma_X \le X \le \Gamma_X,\ 0 < Y \le \Gamma_y, \Psi = 0, \xi = -\nabla^2 \Psi, \frac{\partial \Theta}{\partial n} = 1 \quad (6)$$

Where ltp is a linear time profile. The dimensionless heat transfer across the fluid is presented by the overall Nusselt number < Nu > which is computed, at each boundary, averaging the corresponding local Nusselt number Nu, defined at any point of the physical domain by:

$$Nu_X = U\,\Theta - \frac{\partial \Theta}{\partial X} \text{ and } Nu_Y = V\,\Theta - \frac{\partial \Theta}{\partial Y} \quad (7)$$

The numerical computation of the non dimensional heat flux has been performed integrating the local Nusselt number, at each boundary area. The integrals are approximated by the trapezoidal rule. The heating is a monotonic function of time which is introduced into the governing equations by means of a time dependent Rayleigh number $Ra(t)$. In order to simulate as closely

as possible a real experiment, the calculation starts with a linear temperature profile between hot and cold wall and the fluid at rest.

$$\text{At } t = 0 \quad U(X,Y) = V(X,Y) = 0\,; \quad \Theta(X,Y) = \text{ltp}\,; \quad Ra(t) = 0 \qquad (8)$$

3. Numerical procedure

The equations were solved by solved using the FLEXPDE software. To ensure accurate results, non-uniform meshes of 31×31, 51×31, 71×31 and 31×51 have been employed. Time step $\Delta\tau$ used in calculation varied between 0.1 and 0.01 which require around 100 time steps to 600 time steps for a steady state solution. To ensure convergence at each time step, the iterative process starts from an arbitrary vorticity field, the stream function is found from equation (2) and the velocity field and the vorticity at the walls are calculated. The energy equation (3) is solved and the vorticity discretized equation coefficients calculated with corresponding residual being determined when the tolerance of 10^{-5} is obtained. The Nusselt number is calculated from the temperature and velocity field obtained at the end of the iterative process.

4. Results and discussion

At low Rayleigh number ($Ra = 10^3$), the flow and thermal fields correspond to the pure conduction. The convection is very weak and the flow pattern consists of unicellular streamlines with $|\Psi_{max}| \approx 8.53$ (figure 2). As time progresses, the Rayleigh number increases and the convective heat transfer becomes more important at supercritical Rayleigh number $Ra = 10^5$. The flow tends to occupy more uniformly the whole cavity, as the center of cell moves steadily towards the cooled wall. However, the isotherms do not reach the cavity right side not even for the maximum value of Rayleigh number ($Ra = 10^6$). On the other hand, two rotating rolls with an ascending flow between them are found. Figure 3 shows the overall Nusselt number $< Nu >$ at the top heated boundary plotted against time. In the transient part of this graph there is an almost fixed region where $< Nu > = 1$ indicating a pure conductive thermal regime which starts at approximately the same point for all Ra with the exception of the case $Ra = 10^3$ (large extended pure conductive regime). The influence of the Rayleigh number and the ratio Lx / Ly on the average Nusselt number is shown in Figure 4. One can notice that the law $< Nu > \approx Ra^{1/4}$ is observed for $Ra \geq 10^5$, irrespective of the ratio Lx / Ly. For pure conduction, it may be noticed how the Nusselt number varies in a way close to the inverse of ratio ($< Nu > \approx (Lx / Ly)^{-1}$). It is almost invariant for $Ra = 10^4$ and increases for $Ra > 10^4$, where it varies close to $(Lx / Ly)^{1/4}$ for $Ra = 10^6$. Figure 5 shows isotherms and streamlines for Lx / Ly = 0.25, 0.5, 2, 4 and 5. the flow pattern consists of a counterclockwise cell. It may be noticed that, for all cases, the center of the cell migrates from the heated side to the cooled side when the Rayleigh number increases. For the isotherms, the temperature gradient increases monotonically in the X- direction, and consequently the increase of the circulation, the heated fluid returning after changing its direction tends to fill the whole part of the cavity enhancing the temperature gradient near the cooled wall.

5. Conclusion

A study of Rayleigh-Bénard convection in curvilinear cavity heated upside and symmetrically cooled from curvilinear sides has been studied numerically for arrange of values of the aspect ratio Lx / Ly. For all Rayleigh number, two single roll structures are found. In these ranges of

Rayleigh numbers, transitions between conductive to convective laminar flow structures are observed. At high Rayleigh numbers (Ra = 10^6), for all aspect ratio cavities, time-average vortex ring structures near horizontal and curved walls are found. The recirculation of instantaneous large-scale persistent vertical currents, occurring near the sidewalls, is producing these structures. It can be seen that the effect of the Lx / Ly ratio on the Nusselt number and the maximum stream function value increases with the Rayleigh number.

References

1.K. Stork and U. Müller, 1975, Convection in boxes : an experimental investigation in vertical cylinders and annuli. *J. Fluid Mech.*, n° 71(2), pp. 231-240.
2. K.T. Yang, 1988,Transitions and bifurcations in laminar buoyant flows in confined enclosure. *J. Heat Transfer*, n° 110, pp. 1191-1204.
3.M. P. Arroyo and J. M. Saviron, 1991, Rayleigh-Bénard convection in a small box : spatial features and thermal dependence of the velocity field. *J. Fluid Mech.*, n° 235, pp. 325-348.
4. J. B. Swift, P. C. Hohenberg, 1989, Rayleigh-Bénard convection with time-dependent boundary conditions. *Phys. Rev. A.*, n° 39(8), pp. 4132-4136.
5. J. Pallares, M. P. Arroyo, F. Grau, X. and Giralt F. (2001) Rayleigh-Bénard convection in a cubical cavity: experimental and numerical flow topologies, Exp. Fluids., 31(2), 208-218.
6. M. Cappelli d'Orazio, C. Cianfrini, M. Corcione, 2004, Rayleigh-Bénard convection in tall rectangular enclosure. *International Journal of Thermal Science*, n°43, pp.133-14.
7. H.M. Park, Y.M. Yeo, 2006, Rayleigh-Bénard convection in two dimensional arbitrary finite domains. International Journal of Thermal Science, n°45, pp. 697-705.
8. N. Ouertatani, N. Ben Cheikh, B. Ben Beya, T. Lyli, 2008,Numerical simulation of two dimensional Rayleigh-Bénard convection in an enclosure. *Comptes Rendus Mécanique*, n°336, pp. 64-470.

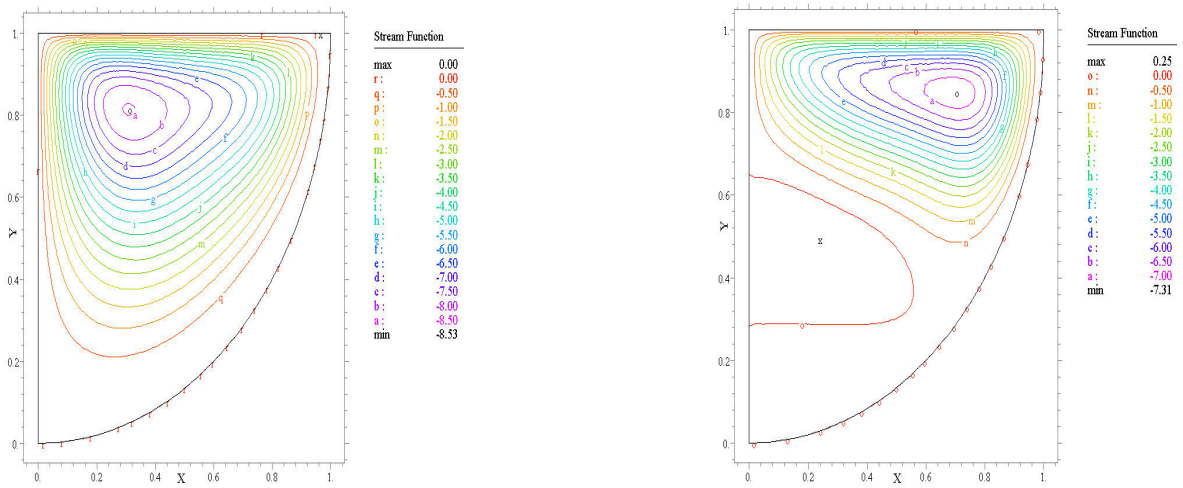

Figure 2: Temporal evolution of the stream function in a curvilinear cavity. Lx / Ly =1. (a) Ra = 10^3, t = 15 min, $|\Psi_{max}| \approx 8.53$. (b) Ra = 10^6, t = 150 min, $|\Psi_{max}| \approx 7.31$.

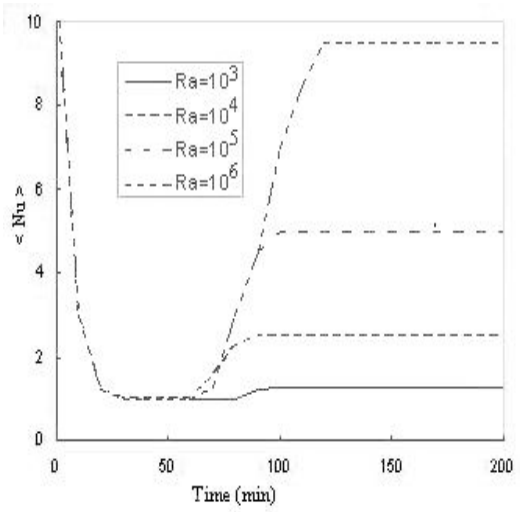

Figure 3: Overall Nusselt number < Nu > as a function of time t inside the cavity Lx / Ly = 1

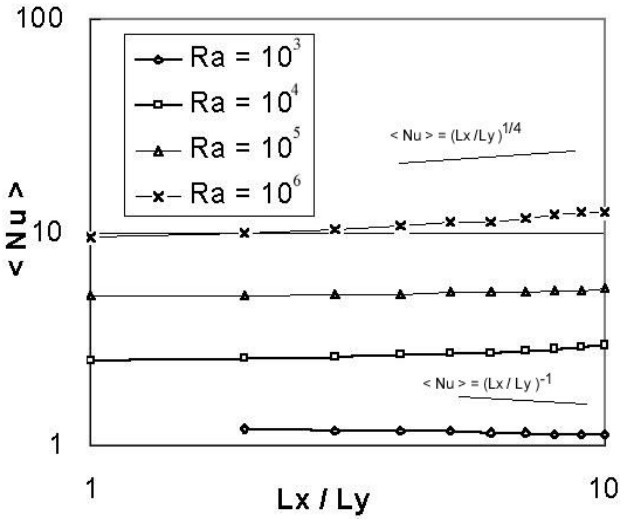

Figure 4 : Overall Nusselt number < Nu > versus the aspect ratio

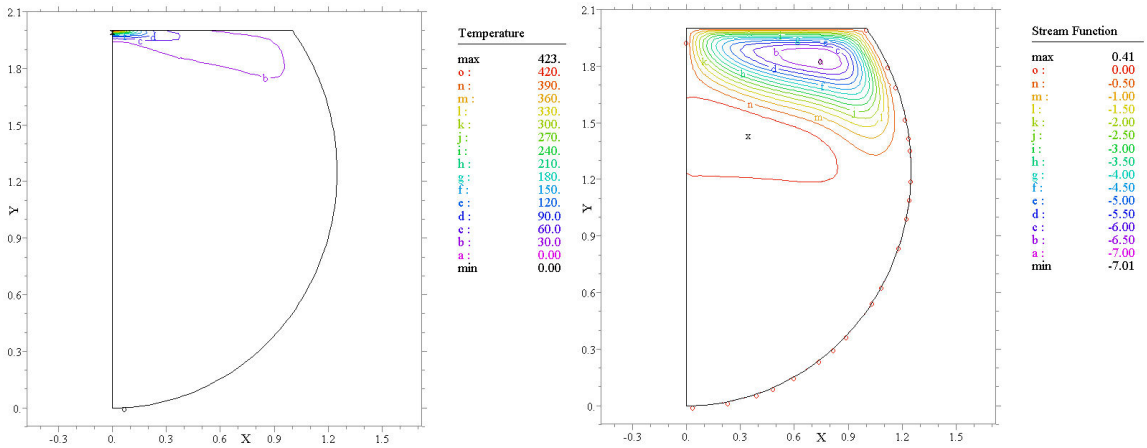

Figure 5: Steady state isotherms (left) and streamlines (right) for a Rayleigh number Ra = 10^6 inside cavity with different aspect ratios. Lx / Ly = 0.2